Characterization of Ag and Ba-modified manganese oxide catalysts: unraveling the factors leading to their enhanced CH_4 oxidation activity

Xiang Wang*† and You-chang Xie

Institute of Physical Chemistry, Peking University, Beijing, 100871, P. R. China

Received (in Montpellier, France) 1st February 2001, Accepted 2nd April 2001
First published as an Advance Article on the web 1st June 2001

Catalysts based on manganese oxide and modified with Ag (AgMn0.10) or Ba (BaMn0.10) were prepared and applied to CH_4 deep oxidation. The catalysts were characterized by means of N_2-BET, XRD, XPS, CH_4-TPR and O_2-TPD techniques. Catalytic evaluation results show that both AgMn0.10 and BaMn0.10 exhibit higher CH_4 oxidation activity than the unmodified MnO_x. However, comparative studies on CO oxidation reveal that only AgMn0.10 displays markedly improved activity for this reaction; the activity of BaMn0.10 remains unchanged compared to unmodified MnO_x. In AgMn0.10, a large amount of more mobile and reactive oxygen species is formed, which is thought to be the main reason for its enhanced CH_4 and CO oxidation activity. Whereas, in BaMn0.10, it is found that the mobility of the lattice oxygen is not increased, but somewhat decreased, thus resulting in no enhanced CO oxidation activity on this catalyst. However, the basicity of the lattice O^{2-} is thought to be increased *via* Ba addition, which is favorable for the activation and rupture of the first C–H bond in CH_4, the rate-determining step for this reaction. Indeed, this modification effect of Ba is believed to be the predominant factor responsible for the enhanced CH_4 oxidation activity of BaMn0.10.

CH_4, the main component of natural gas, is an attractive alternative fuel due to its high H to C ratio, low SO_x and NO_x emissions and its ready availability around the world.[1–3] However, CH_4 is reported to be a much stronger greenhouse gas than CO_2.[4] Although the emission of CH_4 from different sources, *e.g.* industry effluents and automobile exhausts, is not specially regulated now, it is expected to be restricted in the near future. Therefore, the utilization of CH_4 to provide energy or its elimination from the atmosphere to reduce air pollution is desirable.

Traditional catalysts used for high temperature combustion of hydrocarbons and volatile organic compounds (VOCs) are supported noble metals such as Pt, Pd, Rh or combinations thereof.[5] Pd-based catalysts are found to be the most active for CH_4 oxidation.[5–8] However, these catalysts are reported not to be active enough for CH_4 deep oxidation at relatively lower temperatures in these applications.[2,3,8] Currently, the search for catalysts applicable to these processes is an important area of research. Furthermore, because of the limited availability of noble metals, over recent years, there has been a trend to develop combustion catalysts with low Pd loading, or without precious metals and based on composite base metal oxides. Manganese oxides have been extensively studied for different reactions.[9–16] Our previous work has shown that the addition of Ag or Ba to high specific surface area MnO_2 significantly enhances the CH_4 deep oxidation activity of the modified catalysts.[17,18] However, the reasons leading to this improved activity are not yet clearly understood. Therefore, the primary objective in this study is to clarify the modification effects of Ag and Ba on manganese oxides, with the expectation that this will provide some directions for further developing catalysts for CH_4 deep oxidation. In an attempt to elucidate the modification effects of Ag and Ba on manganese oxide, CO oxidation was also performed over the samples. The catalysts were characterized by different physicochemical techniques. In this study, the relations between the physicochemical properties of the catalysts and their catalytic activity are discussed.

Experimental

Catalyst preparation

The high specific surface area MnO_2 precursor (265 $m^2\ g^{-1}$) was prepared *via* the stoichiometric reaction of aqueous $KMnO_4$ and $Mn(NO_3)_2$ solutions.[19,20] Typically, 0.24 M $KMnO_4$ solution was dripped into 50% $Mn(NO_3)_2$ which was under stirring. A brown precipitate, which has been proven to be ultrafine α-MnO_2 powder,[21] was rapidly formed. On completion of the reaction, the pH of the mixture is *ca.* 2.0. This mixture was then vacuum filtered and the precipitate washed repeatedly with distilled water, until the water passing through it was neutral. Afterwards, the product was dried at 110 °C overnight and used as the precursor to prepare the catalysts.

Ag–Mn and Ba–Mn binary oxide catalysts with a M/Mn mol ratio (M = Ag and Ba) of *ca.* 0.1 were prepared by impregnating the MnO_2 precursor with a calculated amount of $AgNO_3$ and $Ba(NO_3)_2$ aqueous solution. After evaporation to dryness in a water bath, both of the samples were calcined in static air atmosphere at 600 °C for 4–6 h. The catalysts are denoted AgMn0.10 and BaMn0.10. The unmodified MnO_x was prepared by direct calcination of the MnO_2 precursor under the same conditions.

† Present address: Department of Chemical Engineering, Towne Building, Room 311A, University of Pennsylvania, Philadelphia, PA 19104, USA. E-mail: wangx2@seas.upenn.edu

 DOI: 10.1039/b101116m

Catalyst characterization

Brunauer–Emmett–Teller (BET) surface areas of the samples were measured by nitrogen adsorption–desorption at 77 K with an ST-30 instrument.

XRD patterns were recorded on a BD-90 X-ray diffractometer with Cu-Kα radiation of 40 kV × 20 mA and Ni filter. The scan step was 0.1° with a preset counting time of 4 s.

XPS experiments were carried out on a VG-ESCA-LAB-5 electron spectrometer using Al-Kα radiation (10 kV, 40 mA). The spectra were obtained at ambient temperature with a chamber pressure of 10^{-8} Torr. The surface O/Mn atomic ratios of the catalysts were calculated from the integrated areas of the $Mn_{2p3/2}$ and O_{1s} peaks after the necessary calibration.

CH_4 temperature programmed reduction (CH_4-TPR) was carried out using a CH_4/N_2 (5.5%) gas mixture. The temperature was increased from 24 to 800 °C at a rate of 10 °C min^{-1}. Prior to entering into the catalyst bed, the gas flow was purified with a MnO oxygen trap and a Molecular Sieve 5A H_2O trap. Generally, the catalysts were diluted with quartz powder to 10% (wt). 100 mg of this mixture containing *ca.* 10 mg pure catalyst powder was used for the experiments. The main reaction products in this experiment are H_2O and CO_2; the formation of CO is negligible, as also attested to by Stobbe *et al.*[22] We followed the reaction by measuring the CH_4 consumption with a thermal conductivity detector (TCD). To rule out the effect of the H_2O and CO_2 produced on the signal, an additional Molecular Sieve 5A trap was attached to the outlet of the reactor to adsorb them. When the trap is saturated, the baseline becomes noisy and some negative H_2O or CO_2 peaks can be observed. With this method, we made sure that the obtained profiles are really based on CH_4 consumption, and not perturbed by the products formed.

O_2 temperature programmed desorption (O_2-TPD) was performed on the same set-up used for CH_4-TPR with a ramp of 10 °C min^{-1} using high purity He as the carrier gas (25 ml min^{-1}). Generally, 40 mg pure sample was used here. Prior to the experiment, the samples were calcined again in dry air at 600 °C for 1 h, then cooled down to room temperature, and purged with a high purity N_2 flow for *ca.* 30 min.

Activity evaluation

Catalytic evaluation was carried out in a U-shaped fixed-bed microreactor (i.d. = 6 mm) with a continuous downflow. The samples were pressed under 8 MPa for 2 min to form pellets, then crushed and sieved. Typically, 0.2 ml 40–60 mesh catalysts were used. To avoid channeling, *ca.* 1 ml of porcelain particles of the same size were loaded above the catalyst bed. A blank experiment confirmed the lack of activity of these porcelain particles under the reaction conditions employed. A K-type thermocouple was placed on top of the catalyst bed (in contact with the catalyst) to monitor the reaction temperature. To measure the light-off behavior of the catalysts, all data were collected with ascending temperature. The volume composition of the feed gas was CH_4 1.5%, O_2 18%, balanced by high purity N_2. The total feed flow rate was 70 ml min^{-1} corresponding to a gas hourly space velocity (GHSV) of 21 000 h^{-1}. The reactants and products were analyzed with an on-line 1102G gas chromatograph equipped with a TCD on a Porapak Q column for CH_4 and CO_2, and on a Molecular Sieve 5A column for CH_4 and CO. In order to collect stable and reproducible data, before analysis, the reaction at each temperature over all of the studied catalysts was stabilized for at least 30 min, then 3–5 injections were made. The flow rate of the carrier gas He was 30 ml min^{-1}. CH_4 conversion was calculated from the change in the peak area before and after passage over the catalyst bed.

CO oxidation was performed on the same set-up and with similar methods. Typically, 0.2 ml 40–60 mesh catalysts were evaluated at a GHSV of 21 000 h^{-1} with ascending temperature. The volume composition of the feed gas was 2.5% CO in air balance. The conversion of CO was calculated from the change in the peak area before and after passage over the catalyst bed.

Results

Activity evaluation

CH_4 deep oxidation. Fig. 1(A) shows the light-off curves of CH_4 oxidation over the modified and unmodified catalysts. In this work, CH_4 is considered to be completely oxidized when conversion reaches 98%. Obviously, AgMn0.10 and BaMn0.10 exhibit higher CH_4 conversion than the unmodified MnO_x at the same reaction temperatures, especially below 500 °C. With increasing reaction temperature, the difference in CH_4 conversion between the two modified catalysts and MnO_x becomes less, although the CH_4 conversions over the modified catalysts are still higher. Among the three samples, BaMn0.10 displays the highest CH_4 conversion at a certain temperature. The complete oxidation of CH_4 occurs at 580 °C over MnO_x, while it takes place at 540 °C over the two modified samples.

Both AgMn0.10 and BaMn0.10 were subjected to a 10 h durability test at 540 °C in *ca.* 4% H_2O (results not shown). No deactivation occurred, indicating they are stable catalysts for CH_4 oxidation.

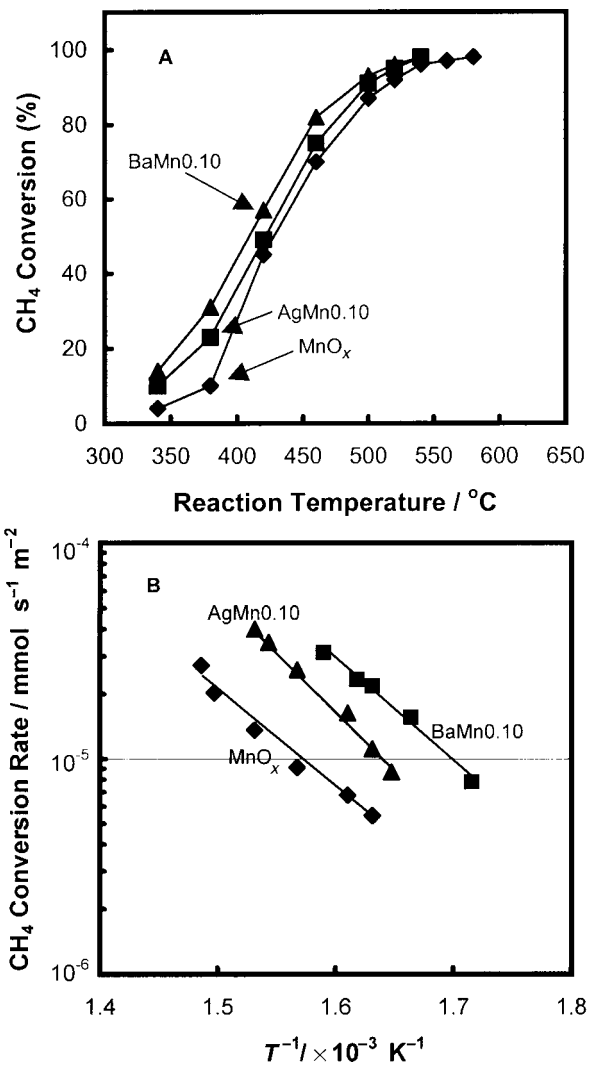

Fig. 1 CH_4 deep oxidation over the catalysts: (A) light-off curves; (B) Arrhenius plots.

The steady-state CH_4 oxidation rates on the three catalysts, which were achieved under differential conditions, are compared in Fig. 1(B) as Arrhenius plots. Apparently, the two modified catalysts show higher activity than MnO_x, as demonstrated by their higher reaction rates. The activation energies on MnO_x, AgMn0.10 and BaMn0.10 are 84, 103 and 94 kJ mol^{-1}, respectively. Considering the results in both Fig. 1(A) and (B), the CH_4 oxidation activity sequence of the catalysts is BaMn0.10 > AgMn0.10 > MnO_x.

CO oxidation. To elucidate the reasons leading to the enhanced CH_4 oxidation activity over the modified catalysts, CO oxidation over the three catalysts was also performed for comparison. The light-off behaviors of CO oxidation over different samples are shown in Fig. 2. Interestingly, although BaMn0.10 displays the highest activity in CH_4 oxidation among the three samples, it does not show improved CO oxidation activity over MnO_x. Both catalysts exhibit nearly the same light-off behaviors, with complete CO oxidation taking place at 140 °C. In contrast, AgMn0.10 shows markedly higher CO oxidation activity than MnO_x and BaMn0.10. It is clear that the steeply ascending light-off curve of AgMn0.10 is separated from those of MnO_x and BaMn0.10 by 30 to 40 °C. The complete oxidation of CO occurs at 90 °C over AgMn0.10, which is 50 °C lower than that on MnO_x and BaMn0.10. Based on steady-state CO oxidation rates under differential conditions, the activation energies on MnO_x, AgMn0.10 and BaMn0.10 are 41, 45 and 46 kJ mol^{-1}, respectively. The ranking of the CO oxidation activities of the catalysts is AgMn0.10 > BaMn0.10 = MnO_x.

N_2-BET and XRD measurements

The specific surface areas of the catalysts are listed in Table 1. The value for MnO_x is 23 m^2 g^{-1}, which is a little higher than that of the two modified samples. Our previous work indicates that the high specific surface area MnO_2 precursor used in this work consists mainly of ultrafine α-MnO_2 powder.[21] Clearly, during the 600 °C calcination, the metastable α-MnO_2 sintered and transformed into more stable crystalline phases, accompanied by a sharp decrease in the surface areas of the samples. It is evident that the surface areas of the modified samples do not play a key role in their enhanced CH_4 deep oxidation activity.

XRD was used to analyze the bulk phase composition of the samples, with the results shown in Fig. 3. For clarity, the crystalline phases detected in each sample are also listed in Table 1. The predominant phase of MnO_x is α-Mn_2O_3 (Bixbyte), together with a trace amount of β-MnO_2 (Pyrolusite). This indicates that part of the lattice oxygen was desorbed from the MnO_2 precursor, with the metastable α-MnO_2 transforming mainly into more stable α-Mn_2O_3 and a trace amount of β-MnO_2.[21] As a result, the oxidation state of Mn decreased from +4 to +3. In AgMn0.10 and BaMn0.10, α-Mn_2O_3 is still one of the main crystalline phases. However, besides this component, some new crystalline phases such as $Ag_2Mn_8O_{16}$, $BaMn_8O_{16}$ and $BaMnO_3$ are clearly detected in the corresponding samples. Obviously, during the calcination, Ag and Ba reacted with the MnO_2 precursor to form these new composite oxides. It is noted that, instead of +3 as in MnO_x, the oxidation state of a considerable amount of the Mn is stabilized at +4 in the two modified samples due to the formation of these composite oxides.

XPS analysis

The surface O/Mn atomic ratios of the samples measured by XPS are listed in Table 1. These ratios are 1.47, 1.75 and 1.61 for MnO_x, AgMn0.10 and BaMn0.10, respectively. Within the experimental error, the O/Mn ratio 1.47 of MnO_x is equal to the calculated ratio of 1.50 for α-Mn_2O_3, the main crystalline phase of this sample, indicating the surface composition of MnO_x is the same as in the bulk. In AgMn0.10, the main components are α-Mn_2O_3 and $Ag_2Mn_8O_{16}$, as evidenced by

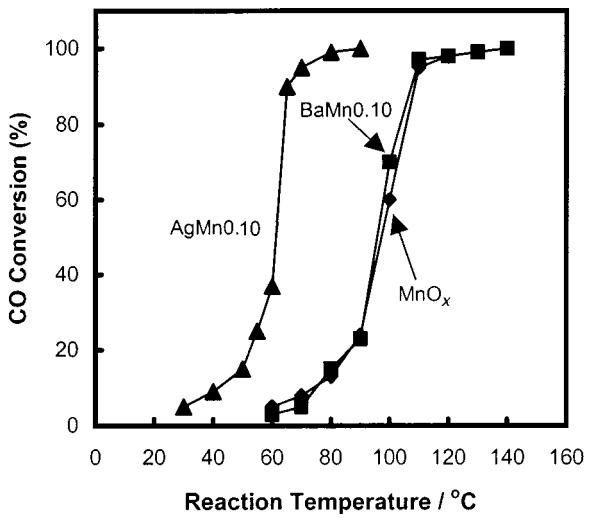

Fig. 2 CO oxidation over the catalysts.

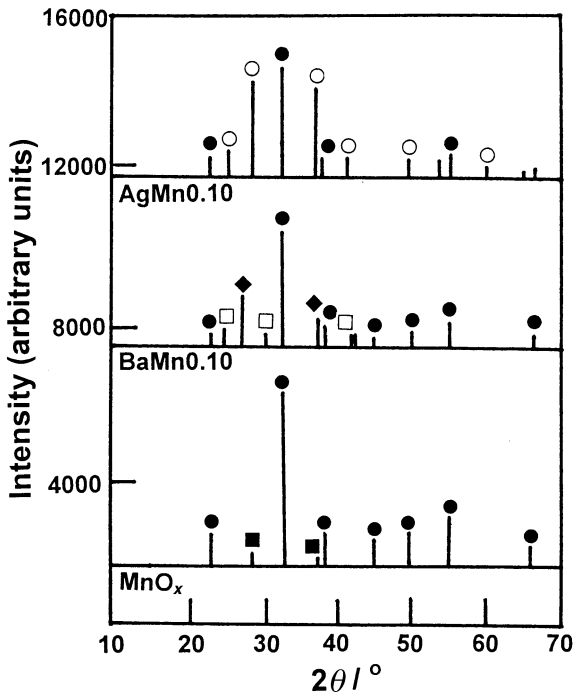

Fig. 3 XRD patterns of the catalysts: (●) α-Mn_2O_3; (■) β-MnO_2; (◆) $BaMn_8O_{16}$; (□) $BaMnO_3$; (○) $Ag_2Mn_8O_{16}$.

Table 1 Physicochemical properties of the catalysts

Catalyst	BET surface area/m^2 g^{-1}	Phase composition (XRD)	Surface O/Mn atomic ratio (XPS)
MnO_x	23	α-Mn_2O_3, β-MnO_2	1.47
AgMn0.10	18	α-Mn_2O_3, $Ag_2Mn_8O_{16}$	1.75
BaMn0.10	20	α-Mn_2O_3, $BaMnO_3$, $BaMn_8O_{16}$	1.61

XRD. The O/Mn ratios of these two crystalline phases are 1.5 and 2.0, respectively. The measured surface O/Mn ratio of AgMn0.10 is 1.75. This implies that both α-Mn_2O_3 and $Ag_2Mn_8O_{16}$ are present on its surface, with slightly more $Ag_2Mn_8O_{16}$ than α-Mn_2O_3. As to BaMn0.10, the O/Mn ratio of 1.61 indicates that the main component of the surface is α-Mn_2O_3. However, a small amount of $BaMn_8O_{16}$ could also be present while the presence of $BaMnO_3$ is negligible since this phase has an O/Mn ratio of 3.0. The non-uniform composition of the two modified samples' surfaces possibly contributes to their enhanced activity for CH_4 oxidation.

CH_4-TPR results

Previous work has substantiated that the formation of more reducible or mobile oxygen species in a catalyst can improve its oxidation activity.[1,23] Therefore, in this study, CH_4-TPR was performed to investigate the nature of the samples (Fig. 4). It is worth noting here that the initial brown color of the samples changed to green after reduction, which is typical for MnO, indicating that this is the main reduction product of the sample.[22,24]

The main reduction peak of MnO_x is located at 605 °C, together with a smaller peak at 500 °C. These two peaks can be assigned to the reduction of α-Mn_2O_3, the main component of this sample, to MnO with Mn_3O_4 as the intermediate.[22] In the profile of AgMn0.10, only a more intense peak is observed at 540 °C, indicating the presence of a greater amount of more reducible oxygen species in this sample than in MnO_x. In comparison, in the reduction curve of BaMn0.10, a wide peak at 530 °C and a narrow peak at 675 °C are found. The CH_4 consumption of the 530 °C peak is less than that of AgMn0.10 and MnO_x in the same temperature region. Overall, the mobility of the lattice oxygen in BaMn0.10 is not improved, but somewhat decreased.

O_2-TPD results

Fig. 5 shows O_2-TPD profiles for the catalysts. All the samples exhibit two oxygen desorption peaks. The two peaks of MnO_x are situated at 425 and 740 °C. The low-temperature peak can be assigned to the desorption of adsorbed oxygen,[11] while the 740 °C peak is attributed to the desorption of lattice oxygen from Mn_2O_3 to form Mn_3O_4.[10]

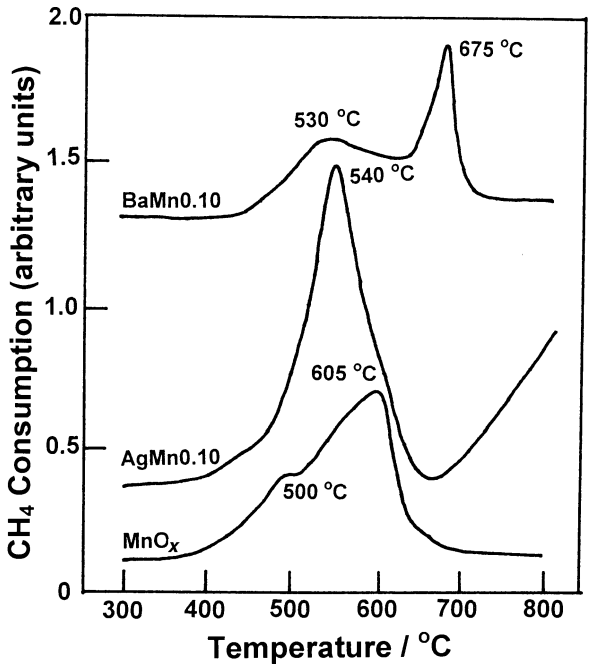

Fig. 4 CH_4-TPR profiles of the catalysts.

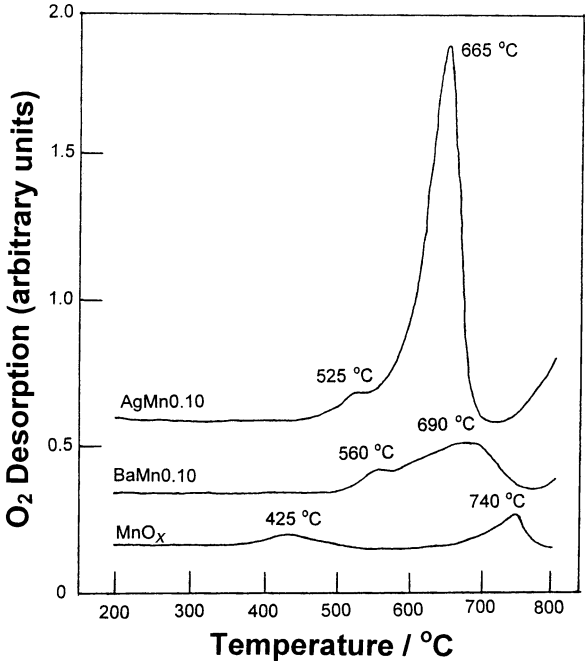

Fig. 5 O_2-TPD profiles of the catalysts.

In comparison, the two oxygen desorption peaks of BaMn0.10 appear at 560 °C and 690 °C. The assignment of these peaks is not very clear, but they are believed to relate to the formation of Ba–Mn composite oxides in the catalyst. The relatively greater total integrated area of the two peaks indicates the amount of desorbed oxygen is larger than in MnO_x. Although CH_4-TPR showed that the reducibility of the major part of the lattice oxygen of BaMn0.10 is not improved, but decreased. This cannot exclude the presence of a small amount of oxygen species that can be desorbed more easily, perhaps due to the non-uniform composition of the catalyst.

Interestingly, AgMn0.10 exhibits a very intense oxygen desorption peak at 665 °C, together with a small shoulder at 525 °C. It is evident that a large amount of a more easily desorbed oxygen species is present in this sample, possibly due to the formation of $Ag_2Mn_8O_{16}$. The presence of a large quantity of more mobile and active oxygen species could be the main reason leading to the exceptional CO oxidation activity of this catalyst.[9–11] Moreover, this could also contribute to its enhanced CH_4 deep oxidation activity.

Discussion

The results in the present work show that both Ag and Ba as additives can improve the activity of manganese oxide for CH_4 oxidation, with the activity sequence being BaMn0.10 > AgMn0.10 > MnO_x. However, for CO oxidation, only Ag can markedly enhance the activity of manganese oxide; Ba does not change the reactivity of the prepared catalyst. This seems to imply that for effective CH_4 and CO oxidation, different functions are required of the catalysts due to the different structures of the CH_4 and CO molecules.

When studying Ag as a catalyst, Sachtler *et al.*[25] found that CO readily reacts with adsorbed oxygen on the surface of metallic Ag. Ag^0 particles or partially oxidized metallic Ag were also proposed by some other authors as active sites for hydrocarbon oxidation.[3,26] However, in this study, although we have no evidence for the absence of Ag^0 crystallites in the samples, neither is there any proof of their presence. It is thus obvious that the enhanced CH_4 and CO oxidation activity of AgMn0.10 cannot be ascribed to the existence of metallic Ag particles.

Kanungo *et al.*[20,27] have studied the physicochemical properties of MnO_2 modified with CuO, namely Hopcalite

catalyst. They attributed the main reason leading to its remarkable CO oxidation activity to the formation of $CuMn_2O_4$ on the surface of this catalyst. The structure of this $CuMn_2O_4$ spinel can be described as $Cu^+[Mn^{3+}Mn^{4+}]O_4{}^{2-}$.[27,28] They suggested that the coexistence of Mn^{3+} and Mn^{4+} in the structure resulted in ready electron transfer between Mn in different oxidation states, since this can occur without the cations changing their positions. As a result, this catalyst shows superior CO oxidation activity.[20,27] Interestingly, in this study, composite oxides such as $Ag_2Mn_8O_{16}$, $BaMn_8O_{16}$ and $BaMnO_3$ are formed in AgMn0.10 and BaMn0.10, respectively. Similarly to $CuMn_2O_4$, both Mn^{3+} and Mn^{4+} are present in $Ag_2Mn_8O_{16}$ and $BaMn_8O_{16}$. On the surface of AgMn0.10, XPS indicates that a considerable amount of $Ag_2Mn_8O_{16}$ coexists with α-Mn_2O_3. Therefore, possibly due to the same inherent reason as Hopcalite catalyst, AgMn0.10 shows also remarkable CO oxidation activity and enhanced CH_4 deep oxidation activity. However, for BaMn0.10, though XPS also shows the coexistence of $BaMn_8O_{16}$ and α-Mn_2O_3 on its surface, the amount of $BaMn_8O_{16}$ is very low. Therefore, it seems that the enhanced CH_4 oxidation activity of BaMn0.10 cannot simply be ascribed to easy electron transfer between Mn^{3+} and Mn^{4+} in the structure.

In the present work, CH_4-TPR and O_2-TPD demonstrated the presence of a large amount of more reducible and mobile oxygen species in AgMn0.10. Indeed, this could relate to the formation of $Ag_2Mn_8O_{16}$ in this sample, and result from the facile electron transfer between Mn^{3+} and Mn^{4+}. The presence of more mobile and reactive oxygen species has been proven previously to be crucial for the significantly enhanced CO oxidation activity of Ag–Mn composite oxide catalysts, which are able to increase the rates of the overall reaction remarkably.[9–11] We thus attribute the enhanced CH_4 and CO oxidation activity of AgMn0.10 to the presence of more mobile and reactive oxygen species in this sample.

However, in this study, there is no proof to show that the mobility of the lattice oxygen of BaMn0.10 is improved; on the contrary, CH_4-TPR results demonstrate that the reducibility and activity is somewhat decreased. This could be the reason why the CO oxidation activity is not enhanced but remains unchanged when compared with MnO_x. In contrast, as mentioned above, BaMn0.10 displays the best CH_4 oxidation activity among the three samples. This seems to imply that the addition of Ba produces some suitable sites or catalytic functions for effective CH_4 oxidation.

CH_4 is well known to be the most difficult to oxidize among all of the hydrocarbons, since the molecule contains only very strong C–H bonds.[1] The fission of the first C–H bond could be the rate-determining step for CH_4 oxidation, and needs high temperature.[29–32] Indeed, the activation of CH_4 should be more difficult than CO on the catalysts, as demonstrated by the higher activation energy of CH_4 as opposed to CO oxidation. When studying CH_4 oxidative coupling, Campbell *et al.*[32] found that the relative activity of rare-earth metal oxides parallels their basicity. It was pointed out that this could be due to the better ability of more basic metal oxides to abstract one hydrogen atom from a CH_4 molecule to form a methyl radical,[32–34] the important intermediate in the reaction. More recently, it has also been suggested that for efficient activation of CH_4 in combustion, highly basic sites are required in a catalyst.[29] Previous work has already demonstrated that the alkalization of metal oxides such as manganese oxides or tin oxide with Li, K or Ba can improve the basicity of their lattice oxygen or form more basic sites.[32–35] We thus speculate that in this study, the predominant reason leading to the enhanced CH_4 oxidation activity of the Ba-modified manganese oxide catalysts could actually be attributed to their improved basicity, which is favorable for the activation of the first C–H bonds in CH_4.

Conclusions

The addition of Ag and Ba to manganese oxide can improve the CH_4 oxidation activity of the resulting catalysts, with the activity sequence BaMn0.10 > AgMn0.10 > MnO_x. However, a comparative study showed that only Ag can markedly enhance the CO oxidation activity of manganese oxide, while the activity of BaMn0.10 is basically unchanged compared to that of MnO_x.

Based on our characterization results, it is believed that the enhanced CH_4 oxidation activity of AgMn0.10 is attributable to the presence of a large amount of mobile and reactive oxygen species, perhaps as a consequence of the formation of $Ag_2Mn_8O_{16}$ in this catalyst. This conclusion is further supported by its superior CO oxidation activity, as previous studies have shown that mobile and reactive oxygen species are critical for effective CO oxidation over a catalyst.

However, the mobility and reactivity of oxygen species are not as crucial for CH_4 oxidation as for CO oxidation, though they are important. The rupture of the first C–H bond of CH_4 is very difficult and generally regarded as the rate-determining step. In this study, it was found that the mobility and reactivity of the oxygen species in BaMn0.10 is not improved over MnO_x, thus resulting in no improvement in the CO oxidation activity of this catalyst. However, the basicity of the lattice O^{2-} can be enhanced *via* Ba addition, which is believed to be favorable for the activation of the first C–H bond in CH_4. It is thus concluded that the CH_4 oxidation activity of BaMn0.10 is markedly enhanced due to this modification effect of Ba.

Acknowledgement

Financial support from the National Science Foundation of China is greatfully acknowledged by the authors.

References

1 Y. Li and J. N. Armor, *Appl. Catal., B*, 1994, **3**, 275.
2 W. S. Epling and G. B. Hoflund, *J. Catal.*, 1999, **182**, 5.
3 Lj. Kundakovic and M. Flytzani-Stephanopoulos, *Appl. Catal. A*, 1999, **183**, 35.
4 E. S. Rubin, R. N. Cooper, R. A. Frosch, T. H. Lee, G. Marland, A. H. Rosenfield and D. D. Stine, *Science*, 1992, **257**, 148.
5 M. M. Zwinkel, S. G. Jaras and P. C. Menon, *Catal. Rev. Sci. Eng.*, 1993, **35**, 319.
6 C. F. Cullis and B. M. Willat, *J. Catal.*, 1983, **83**, 267.
7 R. F. Hicks, H. Qi, M. L. Young and R. G. Lee, *J. Catal.*, 1990, **122**, 280.
8 K. Sekizawa, H. Widjaja, S. Maeda, Y. Ozawa and K. Eguchi, *Appl. Catal., A*, 2000, **200**, 211.
9 S. Imamura, H. Sawada, K. Uemura and S. Ishida, *J. Catal.*, 1988, **109**, 198.
10 M.-F. Luo, X.-X. Yuan and X.-M. Zheng, *Appl. Catal., A*, 1998, **175**, 121.
11 K.-S. Song, S.-K. Kang and S. D. Kim, *Catal. Lett.*, 1997, **49**, 65.
12 M. I. Zaki, M. A. Hasan, L. Pasupulety, N. E. Fouad and H. Knozinger, *New J. Chem.*, 1999, **23**, 1197.
13 M. Baldi, V. S. Escribano, J. M. G. Amores, F. Milella and G. Busca, *Appl. Catal., B*, 1998, **17**, L175.
14 D. Mehandjiev, E. Zhecheva, G. Ivanov and R. Ioncheva, *Appl. Catal., A*, 1998, **167**, 277.
15 G. J. Hutchings, A. A. Mirzaei, R. W. Joyner, M. R. H. Siddqui and S. H. Taylor, *Catal. Lett.*, 1996, **43**, 21.
16 R. Burch, S. Chalker, G. D. Squire and S. C. Tsang, *J. Chem. Soc., Faraday Trans.*, 1990, **86**, 1607.
17 X. Wang and Y. C. Xie, *Fenzi Cuihua*, 1998, **12**, 312.
18 X. Wang and Y. C. Xie, *React. Kinet. Catal. Lett.*, 2000, **71**, 263.
19 E. C. Pitzer and J. C. W. Frazer, *J. Phys. Chem.*, 1941, **45**, 761.
20 S. B. Kanungo, *J. Catal.*, 1979, **58**, 419.
21 X. Wang and Y. C. Xie, *React. Kinet. Catal. Lett.*, 2000, **70**, 43.
22 E. R. Stobbe, B. A. De Boer and J. W. Geus, *Catal. Today*, 1999, **47**, 161.
23 H. Kung and M. Kung, *Adv. Catal.*, 1984, **33**, 159.
24 I. R. Leith and M. G. Howden, *Appl. Catal.*, 1988, **37**, 75.

25 C. Backx, C. P. M. De Groot, P. Biloen and W. M. H. Sachtler, *Surf. Sci.*, 1983, **128**, 81.
26 K. Bethke and H. H. Kung, *J. Catal.*, 1997, **172**, 93.
27 G. M. Schwab and S. B. Kanungo, *Z. Phys. Chem., Neue Folge*, 1977, **107**, 109.
28 A. P. B. Sinha, N. R. Sanjana and A. B. Biswas, *J. Phys. Chem.*, 1958, **62**, 191.
29 R. Burch, D. J. Crittle and M. J. Hayes, *Catal. Today*, 1999, **47**, 229.
30 J. Au-Yeung, K. Chen, A. T. Bell and E. Iglesia, *J. Catal.*, 1999, **188**, 132.
31 V. R. Choudhary and V. H. Rane, *J. Catal.*, 1991, **130**, 411.
32 K. D. Campbell, H. Zhang and J. H. Lunsford, *J. Phys. Chem.*, 1988, **92**, 750.
33 I. A. Kursina, L. N. Kurina, A. I. Galanov and S. I. Galanov, *Catal. Today*, 1998, **42**, 263.
34 S. I. Galanov, L. N. Kurina, A. I. Galanov, A. A. Davydov and V. N. Belousova, *Catal. Today*, 1995, **24**, 293.
35 M. I. Zaki, M. A. Hasan, L. Pasupulety, N. E. Fouad and K. Kumari, *New. J. Chem.*, 1998, **22**, 875.